Spectrally-consistent regularization modeling of turbulent natural convection flows

2012 J. Phys.: Conf. Ser. 395 012123

(http://iopscience.iop.org/1742-6596/395/1/012123)

Spectrally-consistent regularization modeling of turbulent natural convection flows

F Xavier Trias[1], Roel Verstappen[2], Andrey Gorobets[1] and Assensi Oliva[1]

[1] Heat and Mass Transfer Technological Center, Technical University of Catalonia
ETSEIAT, C/Colom 11, 08222 Terrassa, Spain
[2] Johann Bernoulli Institute for Mathematics and Computing Science
University of Groningen P.O. Box 407, 9700 AK Groningen, The Netherlands

E-mail: xavi@cttc.upc.edu, R.W.C.P.Verstappen@math.rug.nl, andrey@cttc.upc.edu, oliva@cttc.upc.edu

Abstract. The incompressible Navier-Stokes equations constitute an excellent mathematical modelization of turbulence. Unfortunately, attempts at performing direct simulations are limited to relatively low-Reynolds numbers because of the almost numberless small scales produced by the non-linear convective term. Alternatively, a dynamically less complex formulation is proposed here. Namely, regularizations of the Navier-Stokes equations that preserve the symmetry and conservation properties exactly. To do so, both convective and diffusive terms are altered in the same vein. In this way, the convective production of small scales is effectively restrained whereas the modified diffusive term introduces a hyperviscosity effect and consequently enhances the destruction of small scales. In practice, the only additional ingredient is a self-adjoint linear filter whose local filter length is determined from the requirement that vortex-stretching must stop at the smallest grid scale. In the present work, the performance of the above-mentioned recent improvements is assessed through application to turbulent natural convection flows by means of comparison with DNS reference data.

1. Introduction

The incompressible Navier-Stokes (NS) equations form an excellent mathematical model for turbulent flows. In primitive variables they read

$$\partial_t u + \mathcal{C}(u,u) = \mathcal{D}u - \nabla p\,; \qquad \nabla \cdot u = 0, \tag{1}$$

where u denotes the velocity field, p represents the pressure, the non-linear convective term is defined by $\mathcal{C}(u,v) = (u \cdot \nabla)\, v$, and the diffusive term reads $\mathcal{D}u = \nu \Delta u$, where ν is the kinematic viscosity. Preserving the symmetries of the continuous differential operators when discretizing them has been shown to be a very suitable approach for direct numerical simulation (DNS) (see [1, 2, 3], for instance). However, DNSs at high Reynolds numbers are not feasible because the convective term produces far too many relevant scales of motion. In the quest for a dynamically less complex formulation we consider regularizations [4, 5, 6] of the non-linearity that preserve the symmetry and conservation properties [7]. In this way, the convective production of small scales is effectively restrained in an unconditionally stable manner. In previous works, we restricted ourselves to the $\mathcal{C}_4$ approximation: the convective term in the NS equations (1) is replaced by the following $\mathcal{O}(\epsilon^4)$-accurate approximation $\mathcal{C}_4(u,v) = \mathcal{C}(\overline{u},\overline{v}) + \overline{\mathcal{C}(\overline{u},v')} + \overline{\mathcal{C}(u',\overline{v})}$, where the

prime indicates the residual of the filter, *e.g.* $u' = u - \overline{u}$, which can be explicitly evaluated, and $\overline{(\cdot)}$ represents a self-adjoint linear filter with filter length ϵ. Therefore, the governing equations result to

$$\partial_t u_\epsilon + \mathcal{C}_4(u_\epsilon, u_\epsilon) = \mathcal{D}u_\epsilon - \nabla p_\epsilon; \qquad \nabla \cdot u_\epsilon = 0, \tag{2}$$

where the variable names are changed from u and p to u_ϵ and p_ϵ, respectively, to stress that the solution of (2) differs from that of (1). Note that the $\mathcal{C}_4$ approximation is also a skew-symmetric operator like the original convective operator. Hence, the same inviscid invariants than the original NS equations are preserved. The numerical algorithm used to solve the governing equations preserves the symmetries and conservation properties too. Then, the only additional ingredient is a self-adjoint linear filter [8] whose local filter length is determined from the requirement that the vortex-stretching must stop at the smallest grid scale [9]. The method has already been successfully tested for a variety of configurations [7, 9]. However, two main drawbacks have been observed: (i) due to the energy conservation, the model tends to display an additional hump in the tail of the spectrum and (ii) for very coarse meshes the damping factor can eventually take very small values. These two issues are addressed in the next section.

2. Restoring the Galilean invariance: hyperviscosity effect

The $\mathcal{C}_4$ regularization preserves all the invariant transformations of the original NS equations, except the Galilean transformation. This usual feature of regularizations [10] can be repaired by means of a proper modification of the time-derivative term. With this idea in mind, and following the same principles than in [7], new regularizations have been recently proposed in [11]. They can be viewed as a generalization of the regularizations proposed in [7] where the Galilean invariance is partially recovered by means of a modification of the diffusive term. Shortly, by imposing all the symmetries and conservation properties of the original convective operator, $\mathcal{C}(u,u)$, and canceling the second-order terms leads to the following one-parameter $\mathcal{O}(\epsilon^4)$-regularization

$$\mathcal{C}_4^\gamma(u,v) = \frac{1}{2}((\mathcal{C}_4 + \mathcal{C}_6) + \gamma(\mathcal{C}_4 - \mathcal{C}_6))(u,v). \tag{3}$$

Notice that for $\gamma = 1$ and $\gamma = -1$, $\mathcal{C}_4^\gamma$ becomes respectively the $\mathcal{C}_4$ and $\mathcal{C}_6$ approximations

$$\mathcal{C}_4(u,v) = \mathcal{C}(\overline{u},\overline{v}) + \overline{\mathcal{C}(\overline{u},v')} + \overline{\mathcal{C}(u',\overline{v})}, \tag{4}$$

$$\mathcal{C}_6(u,v) = \mathcal{C}(\overline{u},\overline{v}) + \mathcal{C}(\overline{u},v') + \mathcal{C}(u',\overline{v}) + \overline{\mathcal{C}(u',v')}. \tag{5}$$

proposed in [7]. Then, to restore the Galilean invariance we need to replace the time-derivative, $\partial_t u_\epsilon$, by the following fourth-order approximation: $(\partial_t)_4^\gamma u_\epsilon = \partial_t(u_\epsilon - 1/2(1+\gamma)u_\epsilon'') = \mathcal{G}_4^\gamma(\partial_t u_\epsilon)$, where $\mathcal{G}_4^\gamma(\phi) = \phi - 1/2(1+\gamma)\phi''$. In this case, the new set of PDEs reads

$$(\partial_t)_4^\gamma u_\epsilon + \mathcal{C}_4^\gamma(u_\epsilon, u_\epsilon) = \mathcal{D}u_\epsilon - \nabla p_\epsilon; \qquad \nabla \cdot u_\epsilon = 0. \tag{6}$$

Therefore, the Galilean invariance might be restored by simply setting $\gamma = -1$. However, this approach suffers from several practical drawbacks [11]. Another possibility relies on modifying appropriately other terms, *e.g.* viscous dissipation. The energy equation for (6) becomes

$$\frac{d}{dt}(\|u_\epsilon\|^2 - 1/2(1+\gamma)\|u_\epsilon'\|^2) = (u_\epsilon, \mathcal{D}u_\epsilon) < 0, \tag{7}$$

provided that the filter is self-adjoint, $\|u\|^2 = (u,u)$, and the innerproduct of functions is defined in the usual way: $(a,b) = \int_\Omega a \cdot b d\Omega$. Therefore, the modification of time-derivative term (6) constitutes a dissipation model. Recalling that $(\mathcal{G}_4^\gamma)^{-1}(\phi) \approx 2\phi - \mathcal{G}_4^\gamma(\phi) + \mathcal{O}(\epsilon^6)$, we can obtain an energetically almost equivalent set of equations by modifying the diffusive term

$$\partial_t u_\epsilon + \mathcal{C}_4^\gamma(u_\epsilon, u_\epsilon) = \mathcal{D}_4^\gamma u_\epsilon - \nabla p_\epsilon \qquad \text{where} \quad \mathcal{D}_4^\gamma u = \mathcal{D}u + 1/2(1+\gamma)(\mathcal{D}u')'. \tag{8}$$

In this way, we are reinforcing the dissipation by means of a hyperviscosity term, $1/2(1+\gamma)(\mathcal{D}u')'$. As expected, this basically acts at the tail of the energy spectrum and therefore helps to mitigate the two above-mentioned drawbacks of the original $\mathcal{C}_4$ regularization. Then, to apply the method two parameters still need to be determined; namely, the local filter length, ϵ, and the constant γ. Hereafter this method is referred as $\{\mathcal{CD}\}_4^\gamma$ regularization.

3. Restraining the production of small scales of motion

3.1. Interscale interactions

To study the interscale interactions in more detail, we continue in the spectral space. The spectral representation of the convective term in the NS equations is given by $\mathcal{C}(u,u)_k = i\Pi(k)\sum_{p+q=k}\hat{u}_p q\hat{u}_q$, where $\Pi(k) = I - kk^T/|k|^2$ denotes the projector onto divergence-free velocity fields in the spectral space. Taking the Fourier transform of (8), we obtain the evolution of each Fourier-mode $\hat{u}_k(t)$ of $u_\epsilon(t)$ for the $\{\mathcal{CD}\}_4^\gamma$ approximation[1]

$$\left(\frac{d}{dt} + h_4^\gamma(\widehat{g}_k)\nu|k|^2\right)\hat{u}_k + i\Pi(k)\sum_{p+q=k} f_4^\gamma\left(\widehat{g}_k,\widehat{g}_p,\widehat{g}_q\right)\hat{u}_p q\hat{v}_q = F_k, \tag{9}$$

where $\widehat{g}_k$ denotes the k-th Fourier-mode of the kernel of the convolution filter, $\overline{\hat{u}}_k = \widehat{g}_k\hat{u}_k$. The mode $\hat{u}_k$ interacts with modes whose wavevectors p and q form a triangle, *i.e.* $k = p + q$. Thus, every triad interaction and the k-th mode of the diffusive term are respectively multiplied by

$$f_4^\gamma(\widehat{g}_k,\widehat{g}_p,\widehat{g}_q) = (\tilde{\gamma}f_4 + (1-\tilde{\gamma})f_6)(\widehat{g}_k,\widehat{g}_p,\widehat{g}_q) \qquad \text{and} \qquad h_4^\gamma(\widehat{g}_k) = 1 + \tilde{\gamma}(1-\widehat{g}_k)^2, \tag{10}$$

where $\tilde{\gamma} = 1/2(1+\gamma)$, $f_4(\widehat{g}_k,\widehat{g}_p,\widehat{g}_q) = \widehat{g}_k(\widehat{g}_p + \widehat{g}_q) + \widehat{g}_p\widehat{g}_q - 2\widehat{g}_k\widehat{g}_p\widehat{g}_q$ and $f_6(\widehat{g}_k,\widehat{g}_p,\widehat{g}_q) = 1 - (1-\widehat{g}_k)(1-\widehat{g}_p)(1-\widehat{g}_q)$, where $0 < f_n \leq 1$ $(n = 4, 6)$ and $h_4^\gamma \geq 1$.

3.2. Stopping the vortex-stretching mechanism

Taking the curl of Eq.(8) leads to

$$\partial_t\omega + \mathcal{C}_4^\gamma(u,\omega) = \mathcal{C}_4^\gamma(\omega,u) + \mathcal{D}_4^\gamma\omega. \tag{11}$$

This equation resembles the vorticity equation that results from the NS equations: the only difference is that $\mathcal{C}$ and $\mathcal{D}$ are replaced by their regularizations $\mathcal{C}_4^\gamma$ and $\mathcal{D}_4^\gamma$, respectively. Left-multiplying the vorticity transport Eq.(11) by ω, we can obtain the evolution of $|\omega|^2$. In this way, the vortex-stretching and dissipation term contributions to $\partial_t|\omega|^2$ result to $\omega\cdot\mathcal{C}_4^\gamma(\omega,u)$ and $\omega\cdot\mathcal{D}_4^\gamma\omega$, respectively. In order to prevent the local intensification of vorticity, dissipation must dominate the vortex-stretching term contribution at the smallest grid scale, $k_c = \pi/h$. In spectral space, this requirement leads to the following inequality

$$\frac{\hat{\omega}_{k_c}\cdot\mathcal{C}_4^\gamma(\omega,u)^*_{k_c} + \mathcal{C}_4^\gamma(\omega,u)_{k_c}\cdot\hat{\omega}^*_{k_c}}{2\hat{\omega}_{k_c}\cdot\hat{\omega}^*_{k_c}} \leq h_4^\gamma\left(\hat{g}_k\right)\nu k_c^2, \tag{12}$$

where the vortex-stretching term is given by $\mathcal{C}_4^\gamma(\omega,u)_{k_c} = \sum_{p+q=k_c} f_4^\gamma\left(\widehat{g}_{k_c},\widehat{g}_p,\widehat{g}_q\right)\hat{\omega}_p iq\hat{u}_q$. Note that $f_4^\gamma\left(\widehat{g}_{k_c},\widehat{g}_p,\widehat{g}_q\right)$ depends on the filter length ϵ and, in general, on the wavevectors p and $q = k_c - p$. This makes very difficult to control the damping effect because f_4^γ cannot be taken out of the summation. To avoid this, filters should be constructed from the requirement that the damping effect of all the triadic interactions at the smallest scale must be virtually independent of the interacting pairs, *i.e.*

$$f_4^\gamma(\widehat{g}_{k_c},\widehat{g}_p,\widehat{g}_q) \approx f_4^\gamma(\widehat{g}_{k_c}). \tag{13}$$

[1] Hereafter, for simplicity, the subindex ϵ is dropped.

This is a crucial property to control the subtle balance between convection and diffusion in order to stop the vortex-stretching mechanism. This point was addressed in detail in [8]. Then, the overall damping effect at the smallest grid scale, $H_4(\widehat{g}_{k_c}) = f_4^{\gamma}(\widehat{g}_{k_c})/h_4^{\gamma}(\widehat{g}_{k_c})$, follows straightforwardly (with the condition that $0 < H_4(\widehat{g}_{k_c}) \leq 1$)

$$H_4(\widehat{g}_{k_c}) = \frac{2\nu k_c^2 \hat{\omega}_{k_c} \cdot \hat{\omega}^*_{k_c}}{\hat{\omega}_{k_c} \cdot \mathcal{C}(\omega,u)^*_{k_c} + \mathcal{C}(\omega,u)_{k_c} \cdot \hat{\omega}^*_{k_c}}. \tag{14}$$

3.3. From spectral to physical space

In the previous subsection we applied our analysis on a spectral space. However, the method needs to be applied on a physical domain in $\mathbb{R}^3$. To that end, here we propose to express the overall damping effect, $H_4(\widehat{g}_{k_c})$, as a function of the invariants of the strain tensor, $S(u) = 1/2(\nabla u + \nabla u^T)$. Recalling that the velocity field, u, is solenoidal ($\nabla \cdot u = 0$); $tr(S) = 0$ and the characteristic equation of S reads $\lambda^3 + Q\lambda + R = 0$, where $R = -1/3tr(S^3) = -det(S) = -\lambda_1\lambda_2\lambda_3$ and $Q = -1/2tr(S^2) = -1/2(\lambda_1^2 + \lambda_2^2 + \lambda_3^2)$ are the invariants of S, respectively. We order the eigenvalues of S by $\lambda_1 \leq \lambda_2 \leq \lambda_3$. Let us now consider an arbitrary part of the flow domain Ω with periodic boundary conditions. The innerproduct is defined in the usual way: $(a,b) = \int_\Omega a \cdot b d\Omega$. Then, taking the L^2 innerproduct of (1) with $-\Delta u$ leads to the enstrophy equation

$$\frac{1}{2}\frac{d}{dt}\|\omega\|^2 = (\omega, \mathcal{C}(\omega,u)) - \nu\,(\nabla\omega, \nabla\omega)\,, \tag{15}$$

where $\|\omega\|^2 = (\omega,\omega)$ and the convective term contribution $(\mathcal{C}(u,\omega),\omega) = 0$ vanishes because of the skew-symmetry of the convective operator. Using the results obtained in [12] and following the same arguments than in [13], it can be shown that the vortex-stretching term can be expressed in terms of the invariant R of $S(u)$

$$(\omega, \mathcal{C}(\omega,u)) = -\frac{4}{3}\int_\Omega tr(S^3) d\Omega = 4\int_\Omega R d\Omega = 4\widetilde{R}, \tag{16}$$

whereas the diffusive terms may be bounded in terms of the invariant Q

$$(\nabla\omega, \nabla\omega) = -\,(\omega, \Delta\omega) \leq -\lambda_\Delta\,(\omega,\omega) = 4\lambda_\Delta \int_\Omega Q d\Omega = 4\lambda_\Delta \widetilde{Q}, \tag{17}$$

where $\lambda_\Delta < 0$ is the largest (smallest in absolute value) non-zero eigenvalue of the Laplacian operator Δ on Ω and $\widetilde{(\cdot)}$ denotes the integral over Ω (top-hat filter). This approach was proposed in [14]. However, since it provides an upper bound it requires an accurate estimation of λ_Δ on Ω. The latter may be cumbersome on unstructured grids. Alternatively, it may be (numerically) computed directly from $(\nabla\omega, \nabla\omega)$ or, even easier, by simply noticing that $(\nabla\omega, \nabla\omega) = 4\int_\Omega Q(\omega) d\Omega = 4\widetilde{Q}$. However, from a numerical point-of-view, this type of integrations are not straightforward. Instead, recalling that $\nabla \times \nabla \times u = \nabla(\nabla \cdot u) - \Delta u$ and $\nabla \cdot u = 0$, a more appropriate expression can be obtained as follows

$$(\nabla\omega, \nabla\omega) = -\,(\omega, \Delta\omega) = (\omega, \nabla \times \nabla \times \omega) = (\nabla \times \omega, \nabla \times \omega) = (\Delta u, \Delta u) = \|\Delta u\|^2. \tag{18}$$

Then, to prevent a local intensification of vorticity, *i.e.* $\|\omega\|_t \leq 0$, the inequality $H_4(\widehat{g}_{k_c}) \leq \nu(\Delta u, \Delta u)/(\omega, S\omega)$ must be satisfied. This inequality is the analog to Eq.(14) in physical space. Additionally, the dynamics of large scales should not be significantly affected by the (small) scales contained within the domain Ω, *i.e.* $(\omega, S\omega) < 0$. Hence, to confine the dynamics of small scales suffices to modify the previous inequality by simply taking the absolute value of its

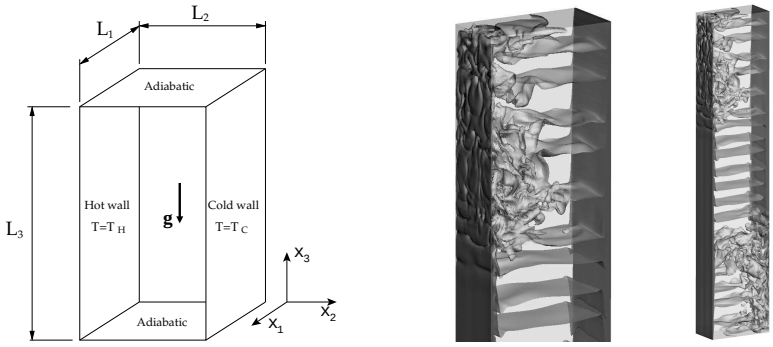

Figure 1. DHC schema (left) and instantaneous isotherms corresponding to the DNS simulation (right).

right-hand-side. Then, from Eq.(16) and recalling that $0 < H_4(\widehat{g}_{k_c}) \leq 1$, a proper definition of the overall damping factor at the smallest grid scale follows

$$H_4(\widehat{g}_{k_c}) = \min\left\{\nu\|\Delta u\|^2/|\widetilde{R}|, 1\right\}. \tag{19}$$

An interesting feature of this model is that it automatically switches off ($R \to 0$) for laminar flows (no vortex-stretching) and 2D flows ($\lambda_2 = 0 \to R = 0$). The near-wall behavior of the invariants is given by $R \propto y^1$ and $Q \propto y^0$, respectively, where y is the distance to the wall. Consequently, it results into a model that switches off in the wall.

4. Performance of $\mathcal{C}_4$-regularization for a turbulent differentially heated cavity

The configuration adopted to illustrate the performance of the $\mathcal{C}_4$-regularization method for turbulent natural convection flows corresponds to an air-filled (Pr = 0.7) differentially heated cavity (DHC) of aspect ratio 5 and Rayleigh number $Ra = 4.5 \times 10^{10}$ (based on the cavity height, L_3). Apart from this, the $\mathcal{C}_4$ method has also been successfully tested for other natural convection configuration. Examples of thereof can be found in [9, 14]. The DNS corresponding to this configuration was carried out on the MareNostrum supercomputer using a $128 \times 318 \times 862$ mesh (the coordinate system is: x_1-spanwise, x_2-horizontal and x_3-vertical, respectively) and presented in [15]. Firstly, we have considered two coarse meshes consisting of $8 \times 14 \times 38$ (RM2) and $8 \times 20 \times 54$ (RM1) grid points, respectively (see Table 1). The meshes are constructed keeping the same grid points distribution as for the DNS but with much coarser spatial resolution. γ_2 and γ_3 are the concentration parameters in the horizontal and vertical directions, respectively (for further details about the mesh generation the reader is referred to [9]). Notice that for the coarsest mesh (RM2) the concentration parameter in the x_2-direction has been slightly modified in order to increase the grid resolution near the vertical walls. The domain size in the periodic direction is the same as for the DNS, *i.e.* $L_1/L_2 = 0.1$. In Table 1, the overall Nusselt number, Nu, together with the maximum and minimum local Nusselt numbers obtained with the coarse meshes RM1 and RM2 are compared with the DNS reference solution. Regarding the Nu, $\mathcal{C}_4$ solutions are able to provide good predictions whereas the results obtained with the same meshes but without any modeling are very far from the reference value $Nu = 154.5$. With regard to Nu_{max} and Nu_{min}, this tendency becomes even more evident. These two quantities are of interest because they occur in two clearly different parts of the vertical boundary layer. Maximum values occur in the upstream part of the boundary layer where it is still almost laminar whereas minimum values are observed at the most downstream part of the boundary layer where it has become fully turbulent (see Figure 1, right). In order to confirm the reliability of the model on coarse grids, the same DHC problem has been solved on a series of 50 randomly generated meshes where the number of grid points varies within the limits: $8 \leq N_1 \leq 12$,

Table 1. The overall, the maximum and the minimum of the averaged Nusselt number.

	DNS	RM1		RM2	
Mesh	$128 \times 318 \times 862$	$8 \times 20 \times 54$		$8 \times 14 \times 38$	
	$\gamma_2 = 2.0$, $\gamma_3 = 0.0$	$\gamma_2 = 2.0$, $\gamma_3 = 1.0$		$\gamma_2 = 2.3$, $\gamma_3 = 1.0$	
		No model	$\mathcal{C}_4$	No model	$\mathcal{C}_4$
Nu	154.5	223.8	**153.4**	207.7	**152.3**
Nu_{max}	781.5	520.6	709.4	500.4	680.0
Nu_{min}	10.5	60.4	7.1	71.0	6.1

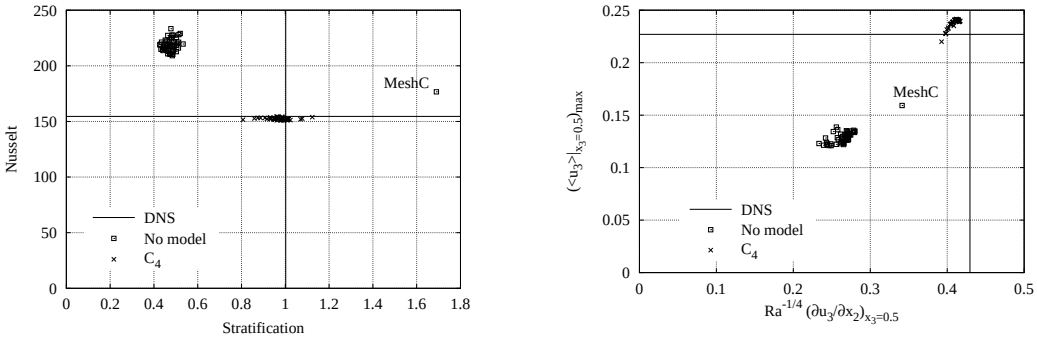

Figure 2. Left: The overall Nusselt number and the centerline stratification. Right: The maximum vertical velocity and the wall shear stress scaled by $Ra^{-1/4}$ at the horizontal mid-height plane.

$16 \leq N_2 \leq 28$ and $44 \leq N_3 \leq 70$, respectively. The concentration parameters, γ_2 and γ_3 are the same than those used for the mesh RM1 (see Table 1). The number of grid points in each direction has been randomly generated irrespectively of the number of points in the other two directions; therefore, some of the numerical experiments correspond to highly skewed meshes. Results for the overall Nusselt and the centerline stratification are displayed in Figure 2 (left). The very good prediction of Nu for all the tested configurations is remarkable; in contrast, the results obtained without modeling substantially differ from the reference solution. Even more important is the fairly good prediction of the stratification. Notice the inaccuracy of the results obtained with a relatively fine mesh of $32 \times 80 \times 216$ (MeshC) grid points. Similar behavior is observed in Figure 2 (right) where the results for the maximum vertical velocity and the wall shear stress at the horizontal mid-plane, $x_3 = 0.5$, are displayed. These two quantities provide valuable information about whether the boundary layer is correctly captured by the model. The $\mathcal{C}_4$ solutions predict quite well the $(0.430, 0.227)$ reference solution whereas both quantities are clearly under-predicted when the model is switched off. This behavior can also be observed in the averaged vertical velocity profile displayed in Figure 3 (left). For the results obtained without modeling, the vertical boundary layer is too thick, whereas with the $\mathcal{C}_4$ regularization, the solutions obtained with the meshes RM1 and RM2 agree well with the DNS solution. It is noticeable that even for a relatively fine mesh results without model are still far from the reference solution. Figure 3 (right) depicts essentially the same for the averaged temperature.

5. Concluding remarks and future research

Since DNSs simulations are not feasible for real-world applications the $\{\mathcal{CD}\}_4^\gamma$-regularization of the NS equations has been proposed as a simulation shortcut: the convective and diffusive operators in the NS equations (1) are replaced by the $\mathcal{O}(\epsilon^4)$-accurate smooth approximation given by Eq.(3) and Eq.(8), respectively. The symmetries and conservation properties of the original convective term are exactly preserved. Doing so, the production of smaller and smaller scales of motion is restrained in an unconditionally stable manner. In this way, the new set

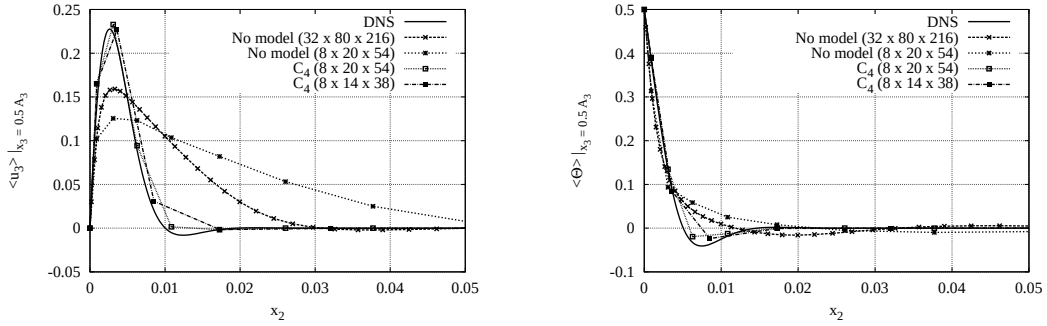

Figure 3. Averaged vertical velocity (left) and temperature (right) profiles at the horizontal mid-height plane. Comparison between the DNS, no-model results obtained with MeshC and $\mathcal{C}_4$ results with meshes RM1 and RM2. Details about the meshes can be found in Table 1.

of equations is dynamically less complex than the original NS equations, and therefore more amenable to be numerically solved. The only additional ingredient is a self-adjoint linear filter whose local filter length is determined from the requirement that vortex-stretching must be stopped at the scale set by the grid. This can be easily satisfied in spectral space via Eq.(14) provided that discrete filter satisfies Eq.(13), *i.e.* the triadic interactions at the smallest scale are virtually independent of the interacting pairs. This was addressed in detail in [8]. However, in physical space it becomes more cumbersome. To circumvent this, here a criterion based on the invariants of the strain tensor is used. Doing so, the expected behavior of a turbulence model is achieved: it switches off (*i.e.* $H_4 = 1$) for laminar flows (no vortex-stretching), 2D flows ($R = 0$) and near the walls. In the present paper, the proposed method has been successfully tested for a turbulent DHC with $\gamma = 0$ of Eq.(8). However, this is not the optimal value of γ. This may be determined by means of a trial-and-error numerical procedure. Alternatively, the constant γ can be approximately bounded by assuming that the smallest grid scale, $k_c = \pi/h$, lies within the inertial range for a classical Kolmogorov energy spectrum $E(k) = C_K \varepsilon^{2/3} k^{-5/3}$. Doing so, the bound $\tilde{\gamma} \gtrsim 4(8C_K^{-3/2} - 1)$ where $\tilde{\gamma} = 1/2(1+\gamma)$ and C_K is the Kolmogorov constant was determined in [16]. Preliminary simulations for homogeneous isotropic turbulence presented in [16] seems to point towards the adequacy of this bound. To confirm this result for a broader variety of test-cases is part of our future research plans.

5.1. Connections between regularization and large-eddy simulation (LES)

Although formally derived from different principles, regularization and LES equations share many features and objectives. Both approaches aim to reduce the dynamical complexity of the original NS equations resulting into a new set of PDE that are more amenable to be numerically solved on a coarse mesh. Shortly, LES equations result from filtering the NS equations in space

$$\partial_t \overline{u} + \mathcal{C}(\overline{u}, \overline{u}) = \mathcal{D}\overline{u} - \nabla \overline{p} - \nabla \cdot \tau(\overline{u}) \; ; \qquad \nabla \cdot \overline{u} = 0, \tag{20}$$

where $\overline{u}$ is the filtered velocity and $\tau(\overline{u})$ is the subgrid stress tensor and aims to approximate the effect of the under-resolved scales, *i.e.* $\tau(\overline{u}) \approx \overline{u \otimes u} - \overline{u} \otimes \overline{u}$. Regularizations of the non-linear convective terms basically reduce the transport towards the small scales by damping the first term in the right-hand-side of the enstrophy equation (15). On the other hand, LES models enhance dissipation. For instance, an eddy-viscosity model, $\tau(\overline{u}) = -2\nu_t S(\overline{u})$, adds the dissipation term $(\nabla\overline{\omega}, \nu_t \nabla\overline{\omega})$ to the enstrophy equation. Then, the turbulent viscosity, ν_t, would result from a simple balance in order to prevent the local intensification of vorticity, $\|\overline{\omega}\|_t^2 \leq 0$,

$$\nu_t = \max\left\{ \frac{4|\widetilde{R}| - \nu \|\Delta\overline{u}\|^2}{\|\Delta\overline{u}\|^2}, 0 \right\}. \tag{21}$$

This analysis can be extended further for other differential operators. For instance, $\tau'(\overline{u}) = 2\nu_t' S(\Delta\overline{u})$ and $\tau''(\overline{u}) = -2\nu_t'' S(\Delta^2\overline{u})$, where $\Delta^2 \equiv \Delta\Delta$ is the bi-Laplacian operator, would lead to the following hyperviscosity terms in the enstrophy equation

$$-\left(\nabla\overline{\omega}, \nu_t' \nabla\Delta\overline{\omega}\right) \quad \text{and} \quad \left(\nabla\overline{\omega}, \nu_t'' \nabla\Delta^2\overline{\omega}\right), \tag{22}$$

respectively. Then, following similar reasonings, the values of ν_t', ν_t'' follow

$$\nu_t' = \max\left\{\frac{4|\widetilde{R}| - \nu\|\Delta\overline{u}\|^2}{-(\Delta\overline{u}, \Delta^2\overline{u})}, 0\right\} \quad \text{and} \quad \nu_t'' = \max\left\{\frac{4|\widetilde{R}| - \nu\|\Delta\overline{u}\|^2}{\|\Delta^2\overline{u}\|^2}, 0\right\}. \tag{23}$$

Notice that only ν_t has dimensions of viscosity. Hence, three eddy-viscosity-type LES models have been obtained by simply considering the balance between the vortex-stretching and the dissipation term in the enstrophy equation (15). Namely, (i) $\tau(\overline{u}) = -2\nu_t S(\overline{u})$, (ii) $\tau'(\overline{u}) = 2\nu_t' S(\Delta\overline{u})$ and (iii) $\tau''(\overline{u}) = -2\nu_t'' S(\Delta^2\overline{u})$, where ν_t, ν_t' and ν_t'' are given by Eqs.(21) and (23), respectively. The models switch off ($R \to 0$) for laminar (no vortex-stretching), 2D flows ($\lambda_2 = 0 \to R = 0$) and near the wall ($R \propto y^1$).

The above described models can be related with already existing LES approaches. Firstly, the model (i) is almost the same as the recently proposed QR-model [13]. Essentially, they only differ on the calculation of the diffusive contribution to the enstrophy equation: instead of making use of equality (18) it is bounded by means of the inequality (17), therefore, the turbulent viscosity is given by $\nu_t \propto \lambda_\Delta^{-1}|\widetilde{R}|/\widetilde{Q}$ instead of Eq.(21). Regarding the models (ii) and (iii) they can be respectively related to the well-known small-large and small-small variational multiscale methods [17] by simply noticing that $u' = -(\epsilon^2/24)\Delta u + \mathcal{O}(\epsilon^4)$ (see [18], for instance). Similar arguments can be used to relate the regularization models given by Eq.(8) and $\gamma > 0$ with the "small-small"-type eddy-viscosity model $\tau''(\overline{u}) = -2\nu_t'' S(\Delta^2\overline{u})$ and ν_t'' given by Eq.(23). To test the performance of these new turbulence models are also part of our future research plans.

Acknowledgments

This work has been financially supported by the *Ministerio de Ciencia e Innovación*, Spain (ENE2010-17801) and a Juan de la Cierva postdoctoral contract (JCI-2009-04910) by the *Ministerio de Ciencia e Innovación*. Calculations have been performed on the IBM MareNostrum supercomputer at the Barcelona Supercomputing Center. The authors thankfully acknowledge these institutions.

References

[1] Morinishi Y, Lund T, Vasilyev O and Moin P 1998 *Journal of Computational Physics* **143** 90–124
[2] Vasilyev O V 2000 *Journal of Computational Physics* **157** 746–761
[3] Verstappen R W C P and Veldman A E P 2003 *Journal of Computational Physics* **187** 343–368
[4] Guermond J L, Oden J T and Prudhomme S 2004 *Journal of Mathematical Fluid Mechanics* **6** 194–248
[5] Geurts B J and Holm D D 2003 *Physics of Fluids* **15** L13–L16
[6] Guermond J L and Prudhomme S 2005 *Physica D* **207** 64–78
[7] Verstappen R 2008 *Computers & Fluids* **37**(7) 887–897
[8] Trias F X and Verstappen R W C P 2011 *Computers & Fluids* **40** 139–148
[9] Trias F X, Verstappen R W C P, Gorobets A, Soria M and Oliva A 2010 *Computers & Fluids* **39**(10) 1815–1831
[10] Guermond J L, Oden J T and Prudhomme S 2003 *Physica D* **177** 23–30
[11] Trias F X, Gorobets A, Verstappen R W C P and Oliva A 2011 *13th European Turbulence Conference* (Warsaw, Poland)
[12] Chae D 2005 *Communications in Mathematical Physics* **263**(9) 789–801
[13] Verstappen R 2011 *Journal of Scientific Computing* **49** 94–110
[14] Trias F X, Gorobets A, Pérez-Segarra C D and Oliva A (published online) *Computers & Fluids*
[15] Trias F X, Gorobets A, Soria M and Oliva A 2011 *7th International Conference on Computational Heat and Mass Transfer* (Istanbul, Turkey)
[16] Trias F X, Folch D, Gorobets A and Oliva A 2012 *Conference on Modelling Fluid Flow 2012* (Budapest, Hungary)
[17] Hughes T J R, Mazzei L, Oberai A A and Wray A A 2001 *Physics of Fluids* **13** 505–512
[18] Sagaut P and Grohens R 1999 *International Journal for Numerical Methods in Fluids* **31**(8) 1195–1220